Subtropical Anticyclones and Summer Monsoons

M. J. RODWELL

Hadley Centre for Climate Prediction and Research, Met Office, Berkshire, Bracknell, United Kingdom

B. J. HOSKINS

Department of Meteorology, University of Reading, Reading, United Kingdom

(Manuscript received 13 March 2000, in final form 20 December 2000)

ABSTRACT

The summer subtropical circulation in the lower troposphere is characterized by continental monsoon rains and anticyclones over the oceans. In winter, the subtropical circulation is more strongly dominated by the zonally averaged flow and its interactions with orography. Here, the mechanics of the summer and winter lower-tropospheric subtropical circulation are explored through the use of a primitive equation model and comparison with observations.

By prescribing in the model the heatings associated with several of the world's monsoons, it is confirmed that the equatorward portion of each subtropical anticyclone may be viewed as the Kelvin wave response to the monsoon heating over the continent to the west. A poleward-flowing low-level jet into a monsoon (such as the Great Plains jet) is required for Sverdrup vorticity balance. This jet effectively closes off the subtropical anticyclone to the east and also transports moisture into the monsoon region. The low-level jet into North America induced by its monsoon heating is augmented by a remote response to the Asian monsoon heating.

The Rossby wave response to the west of subtropical monsoon heating, interacting with the midlatitude westerlies, produces a region of adiabatic descent. It is demonstrated here that a local ''diabatic enhancement'' can lead to a strengthening of the descent. Longitudinal mountain chains act to block the westerly flow and also tend to produce descent in this region. Below the descent, Sverdrup vorticity balance implies equatorward flow that closes off the subtropical anticyclone to the west and induces cool upwelling in the ocean through Ekman transport. Feedbacks, involving, for example, sea surface temperatures, may further enhance the descent in these regions. The conclusion is that the Mediterranean-type climates of regions such as California and Chile may be induced remotely by the monsoon to the east.

Hence it can be argued that the subtropical circulation in summer comprises a set of weakly interacting monsoon systems, each involving monsoon rains, a low-level poleward jet, a subtropical anticyclone to the east, and descent and equatorward flow to the west.

In winter, it is demonstrated how the nonlinear interaction between the strong zonal-mean circulation, associated with the winter ''Hadley cell,'' and the mountains can define many of the large-scale features of the subtropical circulation. The blocking effect of the longitudinal mountain chains is shown to be very important. Subsequent diabatic effects, such as a local diabatic enhancement, would appear to be essential for producing the observed amplitude of these features.

1. Introduction

The word ''monsoon'' is derived from the Arabic word ''mausim'' (Webster 1987). For Arab merchant sailors of the past, the defining aspect of the monsoon was the seasonal reversal of winds over the Indian Ocean (cf. Figs. 1a,b), which they used to dominate trade stretching from Mozambique to China (Hourani 1951; Tibbitts 1971). Indian farmers were more directly interested in the monsoon rains that fell during northern summer. The strong column-integrated heating seen over southern Asia in summer (Fig. 2a) is predominantly due to condensational latent heat release that accompanies these summer monsoon rains. Accounting for radiative cooling, the region within the 150 W m^{-2} contour (drawn thickly) receives an average of at least 10 mm of rainfall per day throughout the summer. In winter there is much less precipitation in this region (Fig. 2b). In reality, wind changes over the ocean and precipitation changes over the land are two parts of the same Asian monsoon system. There is scope for considerable interaction between these parts. For example, river runoff alone implies that an oceanic moisture source for the monsoon rains is essential and changes in the low-level circulation over the ocean will affect these rains. Conversely, the intense heating associated with the monsoon

Corresponding author address: Dr. Mark J. Rodwell, Hadley Centre for Climate Prediction and Research, Met Office, London Road, Bracknell, Berkshire, RG12 2SY, United Kingdom.
E-mail: mjrodwell@meto.gov.uk

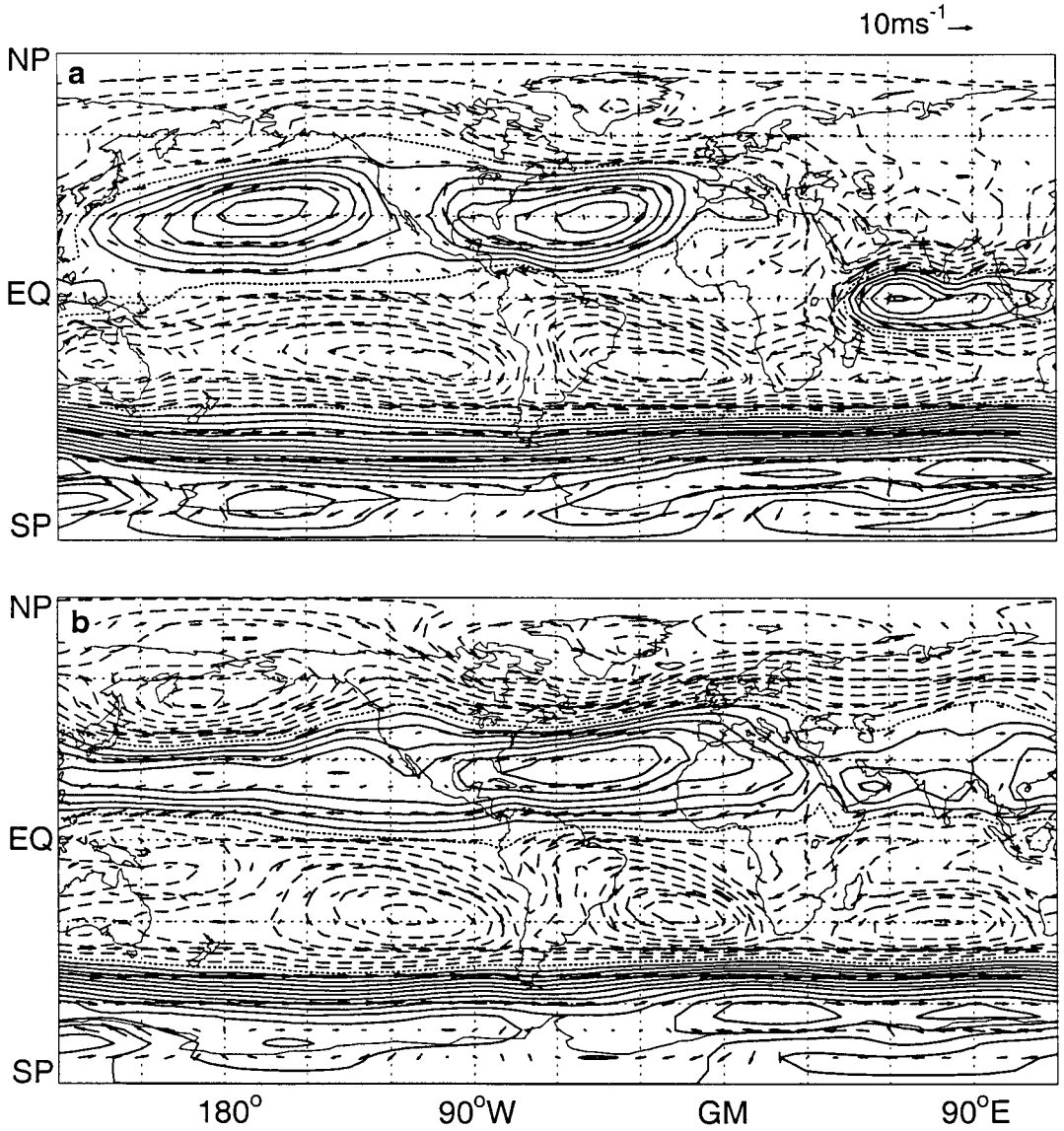

FIG. 1. Mean 850-hPa horizontal winds and streamfunction for (a) 1990–94 Jun–Aug and (b) 1989/90–1993/94 Dec–Feb. Data are taken from analyses from the European Centre for Medium-Range Weather Forecasts (ECMWF). The contour interval is 2×10^6 m^2 s^{-1}. Positive contours are solid, the zero contour is dotted, and negative contours are dashed.

rains is known to modify the circulation over the oceans through the action of Kelvin and Rossby waves (Matsuno 1966; Gill 1980; Heckley and Gill 1984). The dramatic nature of monsoon onset suggests there is a positive feedback between the heating and the low-level circulation.

Monsoon rains throughout the world sustain one-half of the human population. This study considers the role in the large-scale subtropical circulation of monsoon heating over Asia (denoted ''A'' in Fig. 2), the Americas (''NAm'' and ''SAm''), and North Africa (''Naf'').

The low-level circulation over the subtropical oceans is characterized by vast subtropical anticyclones (subtropical highs), which exist year-round and occupy about 40% of the earth's surface. They can be seen in the streamfunction fields shown in Figs. 1a,b, noting that in the Northern (Southern) Hemisphere, an anticyclone appears here as a maximum (minimum) in streamfunction. The wind stress curl associated with the subtropical anticyclones acts to drive the oceanic subtropical gyres (Anderson and Gill 1975) and hence also the warm western boundary currents. On the eastern flanks of the subtropical anticyclones, regions of strong atmospheric descent can be seen (Fig. 3a). Below this descent, and associated with it (Klein and Hartmann 1993; Klein et al. 1995), lie marine status clouds, which, owing to their persistence, low altitude, and high reflectivity, are important for the global radiation budget.

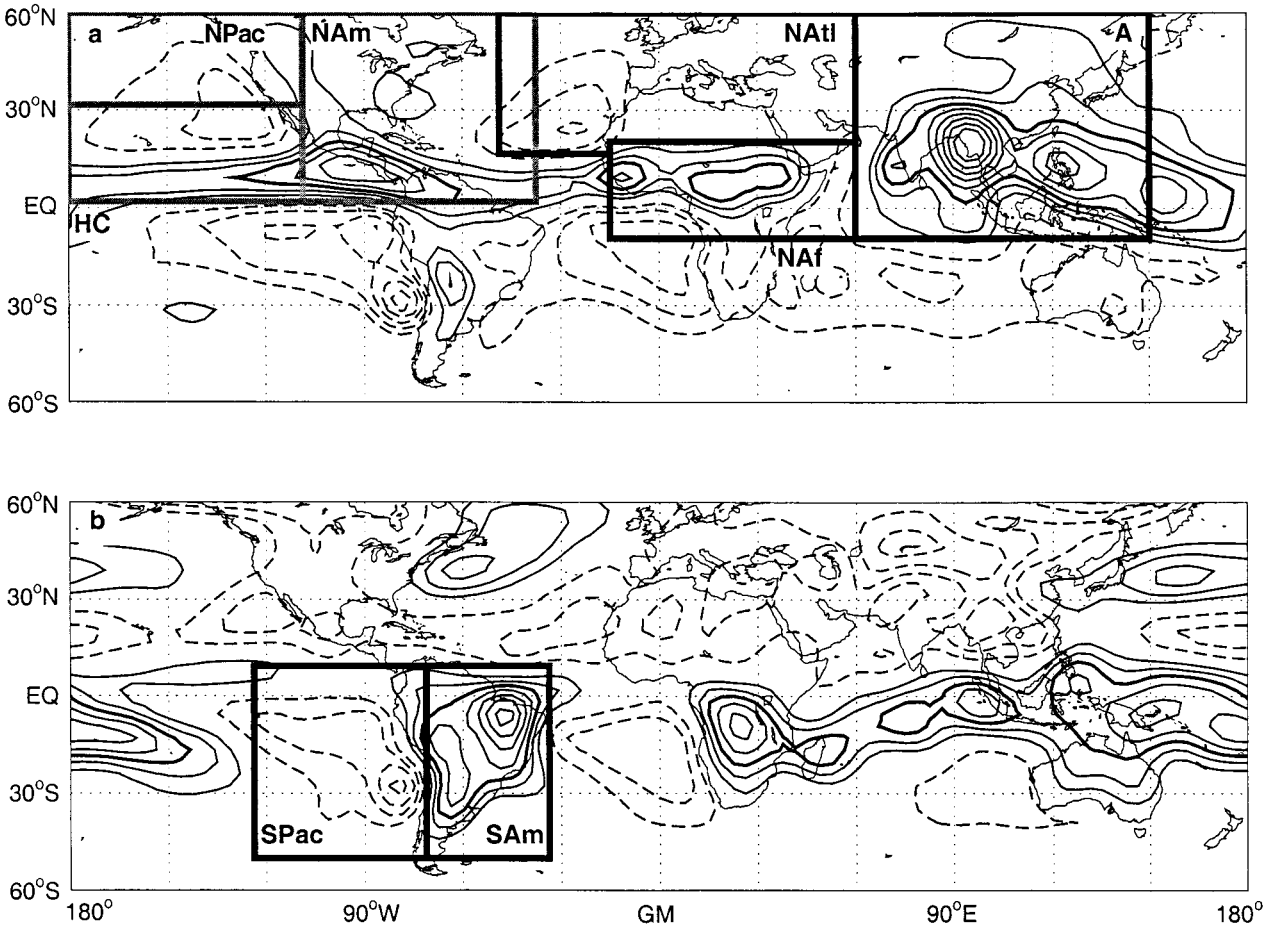

FIG. 2. Column mean heating for (a) Jun–Aug and (b) Dec–Feb calculated as a residual in the thermodynamic energy equation from ECMWF reanalysis data for 1979–93. The contour interval is 50 W m^{-2}. Positive contours are solid, negative contours are dashed, and the zero contour is omitted. Here 150 W m^{-2} contours in the summer hemisphere are shown with thicker lines. The boxes define heating regions for experiments that follow.

In these regions the SSTs are anomalously low, and this is at least partly due to sensible and latent heat fluxes and upwelling forced by equatorward wind stresses. Mean oceanic advection and the radiative effects of the marine cloud also play a role (Ma et al. 1996). Within the subtropical anticyclone regions, evaporation exceeds precipitation by up to 5 mm day^{-1} (Josey et al. 1998), and this may be important for the oceanic thermohaline circulation (Stommel 1961). The subtropical anticyclones also play an important role in the major teleconnection patterns of the globe such as the Pacific–North American pattern and the North Atlantic oscillation and influence the formation and motion of hurricanes. Hence it is clear that both the monsoons and the subtropical anticyclones play a major role in the global circulation of the atmosphere and oceans.

The existence of the subtropical anticyclones has often been attributed to the ''Hadley circulation.'' Held and Hou (1980) showed how the concepts of angular momentum conservation, thermal wind balance, and radiative–convective equilibrium could explain the structure of the annual-mean zonal-mean Hadley circulation. Lindzen and Hou (1988) showed that small meridional displacements of the maximum in zonal-mean surface temperature could lead to the observed large asymmetries in the relative strengths of the summer and winter Hadley cells. They showed how, in the winter hemisphere, there could be strong zonal-mean subtropical descent associated with radiative cooling and a strong equatorially displaced subtropical jet. We will demonstrate how the interaction between this zonal-mean flow and orography can define the basic zonally asymmetric structure of the winter subtropical anticyclones. In the summer hemisphere, Lindzen and Hou (1988) showed how there could be weak or nonexistent subtropical descent. Hence, the Hadley circulation argument would not appear to be appropriate for explaining the summertime existence of the subtropical anticyclones.

Ocean–atmosphere interactions are likely to play a role in the summertime existence of the subtropical anticyclones. The year-round relatively cold sea surface temperatures of the eastern subtropical oceans are likely

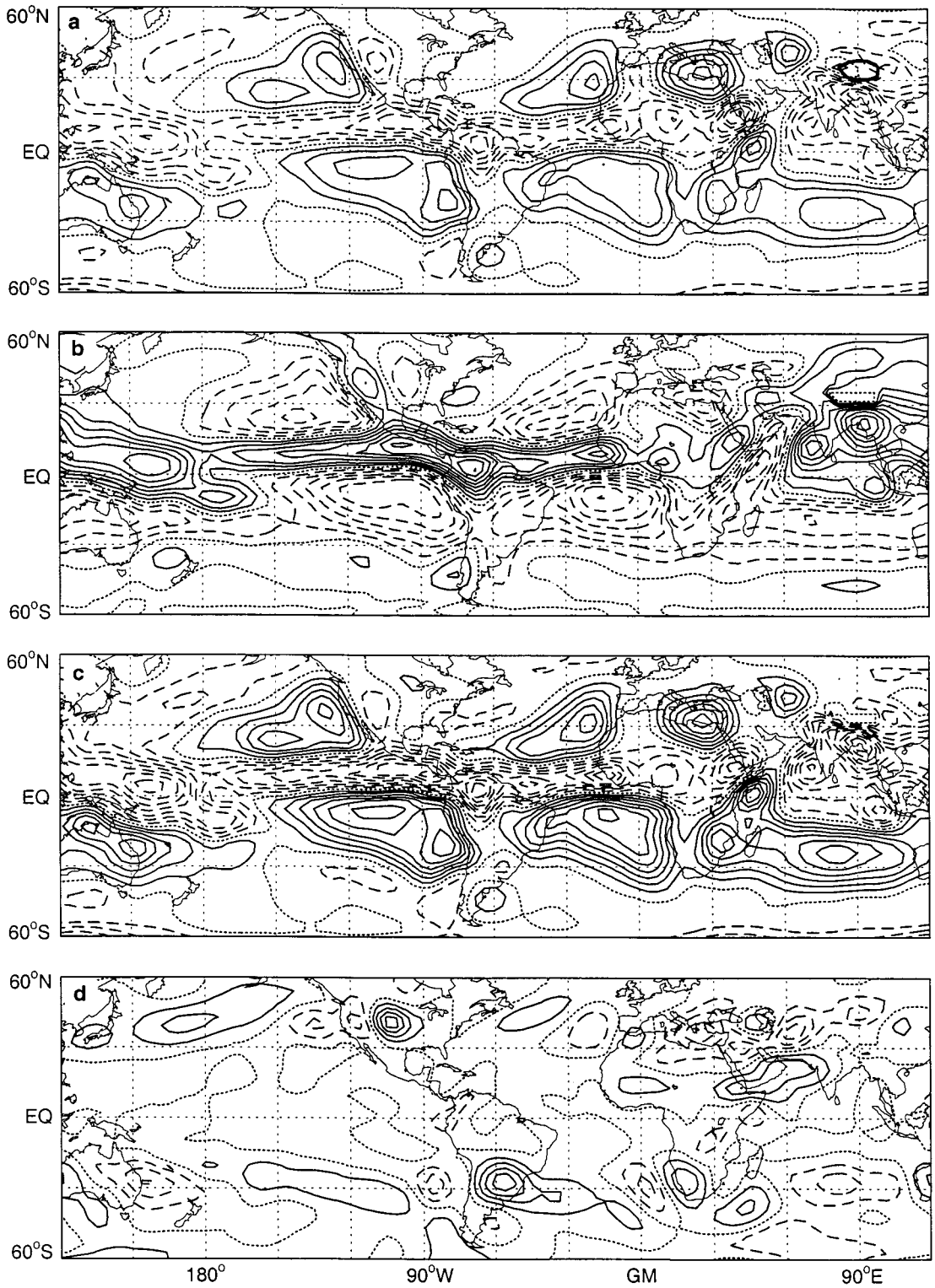

FIG. 3. (a) Jun–Aug mean vertical velocity ω at 674 hPa, with contour interval 0.5 hPa h^{-1}. The following panels show terms in the thermodynamic energy equation calculated at 674 hPa with contour interval 0.5 K day^{-1}: (b) diabatic heating, $\overline{Q}/c_p$; (c) vertical advection, $-(p/p_0)^{\kappa}\overline{\omega}\partial\overline{\theta}/\partial p$; and (d) horizontal advection, $-\overline{\mathbf{v}}\cdot\nabla_p\overline{T}$. The data are taken from analyses for 1990–94 from ECMWF. Positive contours are solid, the zero contour is dotted, and negative contours are dashed.

to reinforce the lack of penetrative convection (e.g., through changes to the moist static energy; Neelin and Held 1987) and thus act to maintain the local atmospheric descent. Conversely, in the time mean, Sverdrup vorticity balance implies that the descent must be accompanied by equatorward winds and hence surface wind stresses that will lead to Ekman pumping of cool waters to the surface (Anderson and Gill 1975). Hence there is the possibility for a positive feedback, and the notion of cause and effect may be problematic.

The summer descent regions on the eastern flanks of the subtropical anticyclones overlap the coastal regions of California and the western Mediterranean (Fig. 3a) and, in December–February, Chile and southwest Africa and Australia. The climates of all these regions can be classified as ''Mediterranean type.'' Rodwell and Hoskins (1996), hereinafter RH, demonstrated that part of the summertime descent over the eastern Mediterranean and Sahara could be induced by forcing an atmospheric primitive equation model with Asian monsoon heating. The monsoon itself was considered to be an inevitable consequence of land–sea contrasts in sensible heating and therefore was taken as a given. The descent was seen as the result of the interaction between the westward-propagating Rossby wave response to the heating and the mean westerly flow on its poleward side. The descent was highly sensitive to the latitude of the heating, being negligible for pre-Asian monsoon heating that is centered nearer the equator at 10°N. Observational evidence from the period of monsoon onset between May and June, which shows a strengthening of descent over the east Mediterranean and Sahara as the monsoon heating moves north, and from paleolake level data for the east Sahara, for example, Lézine and Casanova (1991), provided support for a monsoon–desert mechanism. Mountains were shown to be important for the localization and intensification of descent. The magnitude of the descent forced by the monsoon and mountains was about one-half that observed, and RH argued that this adiabatic descent would imply a reduction in relative humidity and convection and a lowering of the level of radiative emission to space that could lead to a local *diabatic enhancement* of the descent over the eastern Mediterranean and Sahara. In contrast, RH showed that the cooling in the descent region had little or no effect on the Asian monsoon. The question arises as to whether a similar monsoon-forced mechanism is operating over the eastern subtropical oceans and other Mediterranean-type climate regions of the globe. This was the focus of the comments in Hoskins (1996). The previously unanticipated relationship between summer subtropical anticyclones and the monsoon on the continent to their east was highlighted, and some relevant early results from the present study were discussed. Further comments on the processes occurring on the eastern flanks of the subtropical anticyclones were given in Hoskins et al. (1999). However, the more obvious importance of the processes occurring on the western flanks of the summer subtropical anticyclones, where the moist tropical air moves poleward and feeds the monsoon convection, was not discussed.

In this paper the aim is to give a more complete account of the importance of the summer monsoons on the continents to both the east and the west of the anticyclone in determining its properties, and indeed to look at aspects of the whole interacting hemispheric summer monsoon–anticyclone system. As in the previous work we will take the summer monsoon–associated heating as given and use a primitive equation model to assess the features of the tropospheric circulation that are directly related to it.

In section 2, we give a brief description of the model and data. Section 3 discusses concepts and some basic results of this study. Section 4 investigates the Northern Hemisphere summer subtropical circulation with particular reference to the monsoons of North America, Asia, and North Africa. Section 5 investigates the role of the South American monsoon in the Southern Hemisphere summer subtropical circulation. Section 6 considers the wintertime interaction between the mountains and the zonal-mean flow. In section 7, conclusions and a discussion are given.

2. Model and data

Theoretical investigations of the stationary waves usually depend on a linearization about a zonal-mean westerly flow. Such a linearization is clearly questionable for the subtropics, particularly in the summer hemisphere. The June–August zonal-mean winds between 10° and 30°N throughout the troposphere generally lie in the range -5 to $+5$ m s^{-1}. The critical line at which it is zero will clearly play a central role in any linearized, steady-state model. In Hoskins and Rodwell (1995) it was shown that initial value integrations with a primitive equation model gave a realistic nonlinear response to imposed heating fields in the presence of mountains. In particular the low-level monsoon and subtropical anticyclone flows were well simulated. This allowed the study of cross-equatorial flows into the Asian monsoon given in Rodwell and Hoskins (1995) and Rodwell (1997) and the Mediterranean descent in RH. This model will also be used in the present study.

The present investigation has spanned the existence of three climatologies based on analyses from the European Centre for Medium-Range Weather Forecasts (ECMWF). The authors apologize for any unavoidable confusion that this may cause. We refer to, and extend, the results of RH using a climatology based on June–August 1983–88 data. Our initial experiments focusing on the North American monsoon use a 5-yr June–August climatology for the period 1990–94. Subsequently, we test the sensitivity of our North American monsoon results by using the 1979–93 ECMWF reanalyses (ERA; see ECMWF newsletter, September 1996). This ERA dataset is then applied to the monsoons of Asia, North

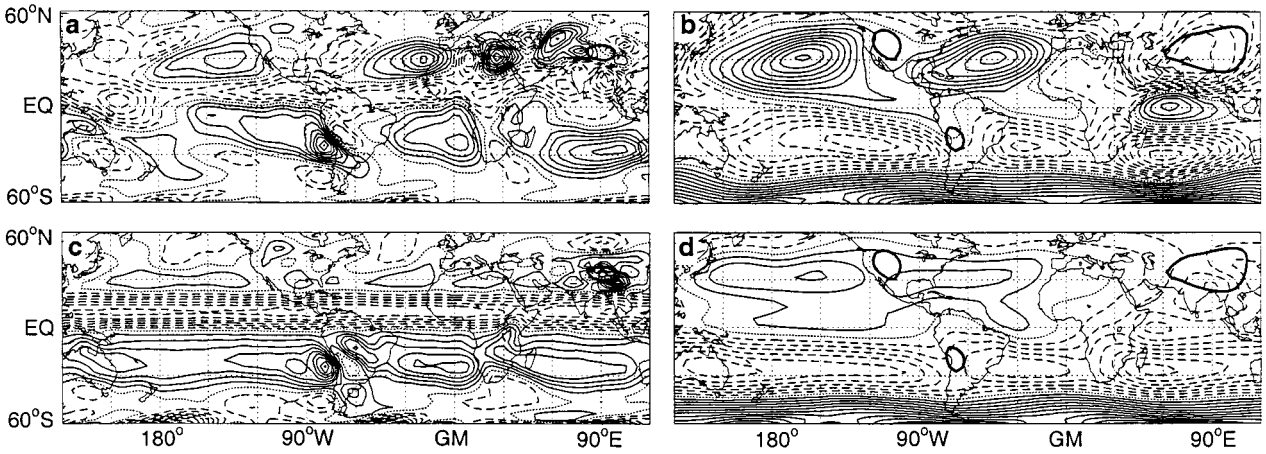

FIG. 4. (a),(c) Vertical velocity, ω, at 674 hPa and (b),(d) horizontal streamfunction at 887 hPa with contour interval 2×10^6 m^2 s^{-1} for Jun–Aug. (a),(b) For the full integration with mountains and ERA Jun–Aug heating. The contour interval for ω is 0.5 hPa h^{-1}. (c),(d) For an integration with mountains only. The contour interval for ω is 0.25 hPa h^{-1}. All results are for day 16. Positive contours are solid, the zero contour dotted, and negative contours dashed. The intersection between the orography and the 887-hPa surface is shown with thick contours.

Africa, and South America. It makes little difference to the conclusions of this investigation into the large-scale subtropical circulation with which climatology we compare our results.

The model used here is discussed in detail by Hoskins and Rodwell (1995). It is a time-dependent, global, hydrostatic, primitive equation model derived from Hoskins and Simmons (1975). It is nonlinear, spectral in the horizontal, and uses finite differences in σ coordinates in the vertical. The horizontal resolution is triangular truncation 31, and there are 15 levels in the vertical. The model includes damping that will be discussed below.

The model is initiated with a zonal-mean climatology. If orography is to be used then this is raised over the first five days of an integration. Hydrostatic adjustments are made to the temperature and surface pressure so that the growing mountains do not unrealistically disturb the atmospheric circulation and so that a near-steady-state solution to topography is achieved as quickly as possible.

At day 5 (day 0 if no orography is used), diabatic forcing is applied as a constant forcing. Depending on the experiment, this forcing is either an idealized field or an ''observed'' field, derived as a residual in the time-mean thermodynamic energy equation (see later). Although the model does not include moisture explicitly, the diabatic forcing mimics, in a noninteractive way, the effects of, for example, latent heat release and radiation budgets. Figures 2a,b showed the total column heating derived in this way for the December–February and June–August seasons, respectively, from the ERA data.

The model uses a linear drag in the lowest two levels, $\sigma = 0.967, 0.887$, on timescales of 1 and 5 days, respectively, over the oceans, and 1/4 and 5/4 days, respectively, over land areas. Unless otherwise specified, Newtonian relaxation toward the basic state (which is also hydrostatically adjusted for orography) is applied with a timescale of 25 days over much of the atmosphere, but decreasing to 5 days in the boundary layer to simulate surface effects. With the exception of the initial adjustments for the growing orography, the zonal averages of vorticity, divergence, temperature, and surface pressure are held constant throughout the integration. This does not in general affect the interpretation of results that are of smaller scale than the latitudinal circle, but a note is made later at the one instance when there may be some impact of this constraint.

The model responds quickly to the orography and diabatic forcing, producing, in the control experiments, a very realistic time-mean atmospheric circulation. For the June–August season, the flow is quasi-steady over the period 5–15 days after the heating is turned on, and we show results for either 10 or 11 days after the heating is applied (i.e., days 15 or 16 in an integration with orography). The precise choice of day has no effect on the conclusions drawn in this paper. After this period of nearly steady flow, midlatitude baroclinic instability produces unsteadiness in the subtropics and Tropics. For the December–February season, the combination in the Northern Hemisphere of strong westerly flow, substantial orography, and heating in the storm tracks leads to earlier instabilities, and, in particular, the circulation over the North Atlantic is less well simulated. For display purposes, and as stated later, we will sometimes show the average of a few days for the December–February simulations, which smooths over some of the synoptic noise. Figures 4a,b show the results for day 16 of the simulation for June–August using ERA data. There is good agreement between Figs. 4a and 3a (ω) and between Figs. 4b and 1a (streamfunction), respec-

tively. The fact that the time-mean flow is well reproduced confirms that the residual method applied to this data gives quite an accurate estimate of the heating. Although the agreement is good, the model in this control simulation mode is somewhat of a consistency check—reproducing the mean flow that was used to calculate the heating applied. It does confirm that the midlatitude transients do not play a dominant role in the structure of the summer subtropical anticyclones. The real benefits of using the model are realized when changes are made to it and sensitivity tests are conducted.

3. Concepts and basic results

a. Thermodynamic balance

Following more limited discussions in RH and in Hoskins et al. (1999), an analysis of the time-mean thermodynamic energy equation is instructive and can, among other things, indicate the maximum amount of remote descent (or ascent) that can be expected to result directly from monsoon and mountain forcing. The time-mean thermodynamic energy equation in pressure coordinates can be written as

$$\underset{\text{A}}{\frac{\partial \overline{T}}{\partial t}} = \underset{\text{B}}{\frac{\overline{Q}}{c_p}} - \underset{\text{C}}{\left(\frac{p}{p_0}\right)^{\kappa} \overline{\omega} \frac{\partial \overline{\theta}}{\partial p}} - \underset{\text{D}}{\overline{\mathbf{v}} \cdot \boldsymbol{\nabla}_p \overline{T}} - \underset{\text{E}}{\left(\frac{p}{p_0}\right)^{\kappa} \frac{\partial}{\partial p} \overline{(\omega' \theta')}} - \underset{\text{F}}{\boldsymbol{\nabla}_p \cdot \overline{(\mathbf{v}' T')}}, \quad (1)$$

where T is temperature, t is time, Q is (diabatic) heating and cooling, c_p is the specific heat of dry air at constant pressure, p is pressure, p_0 is a standard constant pressure, $\kappa = R/c_p$, R is the gas constant for dry air, $\omega =$ vertical velocity Dp/Dt, $\theta = (p/p_0)^{-\kappa}T$ is potential temperature, and $\mathbf{v}$ is horizontal wind velocity. An overbar implies a time mean, and a prime signifies a deviation from the time mean. On the seasonal timescale, the time-dependence term, A, is negligible. June–August data from the 1989/90–1994/95 climatology is used to calculate terms C–F, and term B is derived as a residual. At the horizontal grid resolution used (about 3.75° × 3.75°), and particularly away from the midlatitude storm tracks, we find that the transient terms, E and F, do not play a significant role in the balance. Hence the dominant balance is between the diabatic forcing, B, the mean ''vertical advection of θ,'' C, and the mean horizontal advection, D. As already discussed, Fig. 3a gives the vertical velocity ω for the June–August season at 674 hPa. Figures 3b–d show the three terms, B, C, and D, respectively for this period and for the same level. The diabatic forcing (Fig. 3b) clearly shows latent heating in the ITCZ region just north of the equator, and the monsoons of Asia and North America can be seen as northward extensions of this heating. In contrast, the descent regions over the eastern subtropical oceans are seen as areas of net cooling.

In the Tropics, the predominent balance is between the diabatic term (Fig. 3b) and the mean vertical advection term (Fig. 3c). This reflects a balance between diabatic warming (cooling) and adiabatic cooling (warming) due to ascent (descent) in a local Hadley circulation, particularly over the eastern oceans. A local *summertime* Hadley circulation in the northern Tropics may not contradict the ideas of Lindzen and Hou (1988). This is because cold sea surface temperatures over the eastern subtropical oceans imply strong meridional gradients in radiative–convective equilibrium temperatures and hence the departures from the momentum-based temperature curve that are essential for meridional overturning.

In the subtropics, horizontal advection (Fig. 3d) becomes more important in the thermodynamic balance. Exact cancellation between the vertical advection term (Fig. 3c) and the horizontal advection term (Fig. 3d) would imply vertical motions as air moves along sloping isentropic surfaces. Since, in the subtropical descent regions, the diabatic forcing (Fig. 3b) and horizontal advection (Fig. 3d) terms are of the same sign rather than tending to cancel, the fraction of the total time-mean descent, which can be directly related to adiabatic motions, could be argued to be approximately D/C, as defined in (1). Using this argument, it can be seen from Fig. 3 that about 40% of the total descent over the eastern subtropical North Pacific is ''adiabatic.'' This represents the maximum percentage of descent that could be expected to result directly from remote monsoon and mountain forcing. Generally, for the oceanic descent regions of both summer and winter hemispheres, the percentage is around 30%. For the eastern Mediterranean–Sahara region, the fraction is around 50%. Rodwell and Hoskins (1996) showed that the latter was accounted for by Asian monsoon and mountain forcing and speculated that much of the remaining 50% was a diabatic enhancement to this remotely forced descent. The smaller percentages for the oceanic descent regions could reflect extra positive feedbacks involving air–sea interaction. This study attempts to determine how much of this adiabatic descent is forced by the monsoon and orography to the east and how much of the remaining descent may be viewed as simply a diabatic amplification of it.

Over the western oceans in the western flanks of the North Atlantic and North Pacific subtropical anticyclones there is cool vertical advection (Fig. 3c) and warm horizontal advection (Fig. 3d). Figure 3b shows that there is also heating in these regions. The air here is upgliding in sympathy with, but more steeply than, the isentropes. Over southern Japan for example, the ''adiabatic ascent'' fraction is about 50%. The processes occurring on the western flanks of the subtropical anticyclones will also be discussed here.

b. Basic results

As a means of introduction to some of the salient features of the subtropical circulation, we present a series of idealized experiments in which different factors are successively included.

The first experiment is an integration with no mountains and with idealized elliptical deep-convective monsoon heating centered at 25°N, 90°E and 400 hPa and maximizing at 5 K day^{-1} (as used in RH). The zonal mean initial state is from the 1983–88 data. There is a surface drag applied globally in the lowest and second-to-lowest model levels with timescales of 1 and 5 days, respectively, but there is no Newtonian relaxation applied. Figures 5a,b show longitude–height plots of vertical velocity ω and meridional wind, respectively, at 35°N for day 11 of the integration. Here 35°N is chosen because it cuts through the center of the descent regions seen in Fig. 3a and in the idealized experiments of RH. Ascent is seen in the heating region (Fig. 5a). In this summer situation, with a lack of baroclinicity, the thermodynamic balance here is essentially between the heating term, B, and the vertical advection term, C, in (1).

In agreement with Sverdrup vorticity balance of the steady flow,

$$\beta v \approx f\frac{\partial \omega}{\partial p}, \tag{2}$$

strong poleward flow is seen below the maximum ascent (Fig. 5b, around 100°E). In (2), v is meridional wind, f is the Coriolis parameter, and β is its meridional gradient. For the North American monsoon, this poleward flow is commonly known as the Great Plains low-level jet (LLJ). For the South American monsoon, it is often known as the Pampas LLJ. Because of the continent–ocean distribution and also the topography of eastern Africa (Rodwell and Hoskins 1995), the inflow to the Asian monsoon is a little different, but the main analogous flows would be the Somali jet and its extension northeastward into the Bay of Bengal and the poleward flow over the South China Sea region. To satisfy Sverdrup balance and as an oceanic source of moisture, it is clear that these LLJs are an essential element of any subtropical monsoon system. Part of the flow of the LLJ on the equatorward side of the monsoon will be associated with the local divergent circulation (Neelin and Held 1987) but for the large-scale monsoon and particularly for the subtropical heating regions, the rotational flow associated with the subtropical anticyclone to the east will be important. This is clear from the wind vectors and streamfunction contours shown in Fig. 1 (e.g., at 30°N, 100°W in Fig. 1a and at 20°S, 60°W in Fig. 1b).

Above the ascent maximum, Sverdrup balance also explains the equatorward flow seen at about 200 hPa (Fig. 5b), and hence the location of the upper-level monsoon anticyclone (Sardeshmukh and Hoskins 1988). Figure 5b also shows that the baroclinic westward tilt with height in the heating region becomes more equivalent barotropic in the downstream wave train (Hoskins and Karoly 1981; Held 1983).

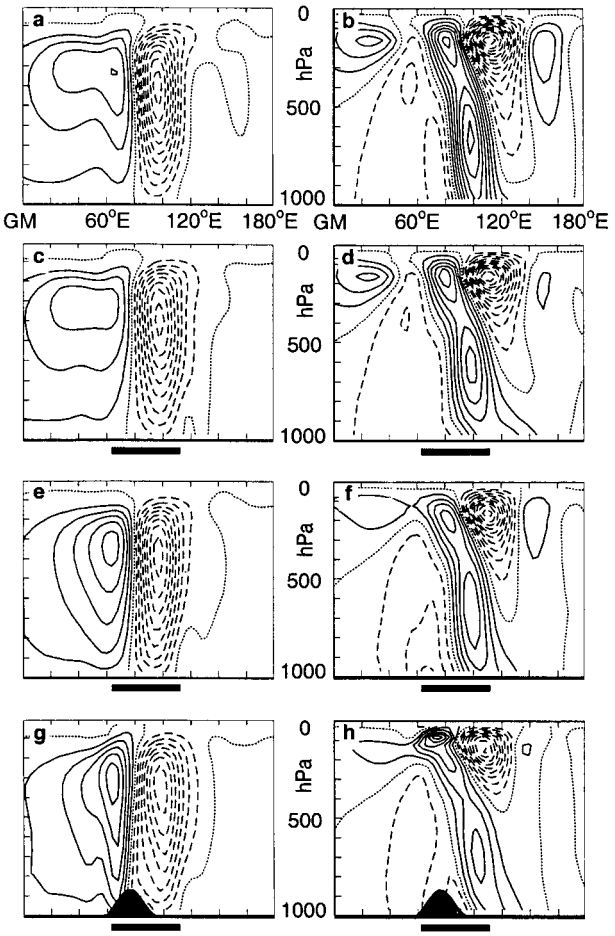

FIG. 5. A sequence of idealized simulations for Jun–Aug in which salient features of a monsoon circulation are successively included. (a),(c),(e),(g) Vertical velocity ω with contour interval 0.25 hPa h^{-1} and (b),(d),(f),(h) meridional wind with contour interval 1 m s^{-1}. (a) and (b) Idealized monsoon heating is applied at 25°N, 90°E. (c) and (d) A continent with a drag coefficient over the land 4 times as strong as over the ocean is added in the box 1.9°–61.2°N and 63.75°–116.25°E—as indicated by the thick horizontal bar. (e) and (f) Newtonian cooling to the basic state is applied with a timescale of 4 days. The monsoon heating is 33% stronger to counteract the Newtonian cooling in the monsoon region and thus to leave net monsoon heating unchanged. (g) and (h) An idealized mountain is included as shown. Horizontally, the mountain is elliptical, and at 887 hPa it extends from 20°–40°N. Results are shown for 11 days after the heating is applied [day 11 for (a)–(f), day 16 for (g) and (h)]. Positive contours are solid, the zero contour is dotted, and negative contours are dashed.

As in RH, descent is seen to the west (and northwest) of the heating center. In agreement with Sverdrup balance, this subtropical descent is accompanied by low-level equatorward flow (Fig. 5b) maximizing at about 75°E. In this idealized experiment, this forms part of the flow along the eastern flank of the subtropical anticyclone to the west.

In the second experiment, an idealized Northern

Hemisphere continent encompassing the monsoon heating region is added. The continent is applied in the box 1.9°–61.2°N and 63.75°–116.25°E, and its effect is felt through a fourfold increase in the drag coefficients at the lowest two model levels. This is the only change made to the previous simulation. The results for day 11 are shown in Figs. 5c,d. The thick line under the longitude axis shows the longitudinal location of the continent. The location of the prescribed heating remains unchanged although in reality continental geometry is likely to affect it (Dirmeyer 1998). The increased surface drag leads to a reduction in the strength of the low-level flow (Fig. 5d) and weaker descent over the western continent (Fig. 5c). To the west, over the ocean, there is a small strengthening of the descent.

Rodwell and Hoskins (1996) argument for the diabatic enhancement of descent was that the adiabatic descent, which has a warm thermal anomaly associated with it, would both inhibit latent heat release and increase radiative cooling. The effect of these changes would be net cooling of the atmosphere and hence a probable increase in the strength of the descent. The observed cooling over the east Mediterranean and Sahara was thought to be due to these factors and possibly, in the longer term, the ''Charney-type'' rainfall–vegetation–albedo–radiation feedback over the desert. In the present investigation, air–sea interactions may give additional enhancing factors.

To demonstrate the diabatic enhancement hypothesis in the third experiment with this simple model, we make use of the thermal anomaly associated with the adiabatic descent and apply Newtonian relaxation of the temperature toward that of the basic state. The timescale for relaxation (4 days) was chosen so that the *implied* damping of the temperature anomaly seen in the descent region for the previous experiment agreed with the rate of cooling seen in observations (Fig. 3a). Four days is a relatively short timescale, but partly this is required because observed *local* temperatures in these descent regions are about 7 K cooler than the zonal mean basic state used here. If one were to use a locally more realistic basic state, then this timescale could be more than doubled. The diabatic forcing term that we arrive at is intended to be a first attempt with this simple model to account for all the possible feedbacks mentioned above. When this Newtonian relaxation is applied without making any other changes to the model, the descent is indeed strengthened by 18%. However, because the relaxation is applied globally, the total heating in the monsoon region is reduced and the ascent there is simultaneously weakened (by 22.3%). Ideally, the monsoon heating and ascent should be kept constant. Figure 5e shows the results from an integration when, additionally, the monsoon heating was increased by 33% to counteract the effect of Newtonian cooling in the monsoon region [$(100-22.3) \times 1.33 = 103\%$, i.e., approximately unchanged]. The monsoon ascent is indeed little changed (it is actually less than 1% stronger), but the descent is significantly strengthened, by 54%, and the low-level equatorward flow is markedly strengthened (Fig. 5f). The descent is still centered at about 35°N.

The height of maximum descent is located at around 350 hPa. The observations for the June–August season show a similar if slightly lower level of maximum descent over the east Mediterranean–Sahara and southwest Asia. However, ''observed'' mean descent over the eastern subtropical North Pacific and Atlantic maximizes at around 700 hPa. One might suspect that this difference is due to the Newtonian relaxation not well representing the vertical profile of the effects of air–sea interaction and low-level marine stratus cloud. Later experimental results will tend to confirm this as being a partial reason for the difference.

Although the 54% strengthening of descent is appreciable, it is not a doubling because the Newtonian relaxation changes the thermal structure of the atmosphere. In reality, the cooling may depend more directly on the large-scale descent than on the thermal state of the atmosphere and hence would not be so prone to this diminishing effect. However, if local cooling was specified in our model as being a function of descent then the result would be highly dependent on the choice of function. For this reason we have not attempted to make such a link although the exercise in finding a function that gave the observed flow may give further insight into the physics of the feedback.

The final experiment in the series shows the effect of including an idealized mountain on the western side of the continent, mimicking the situation in North and South America in particular. This is the only change made from the previous experiment. The descent (Fig. 5g) is little changed overall but becomes more localized above the western slope of the mountain where low-level descent is strengthened. One can speculate that steeper, higher (and more realistic) orography may also lead to a lowering of the level of maximum descent. Low-level Sverdrup balance appears to be somewhat weakened close to this idealized mountain.

The relative effects of heating and orography have been explored in the full model. Figures 4c,d show the results for day 16 of a simulation identical to the full June–August simulation in Figs. 4a,b but with no heating (other than that implied by the maintenance of the zonal mean flow). Note that the contour interval in Fig. 4c is one-half that in Fig. 4a. The *differences* between Figs. 4a,b and Figs. 4c,d emphasize the importance of zonally asymmetric heating, particularly in the summer (Northern) hemisphere. The *similarities* between Figs. 4a,b and Figs. 4c,d are greatest in the winter (Southern) hemisphere, but they are not insignificant in the summer (Northern) hemisphere. These similarities imply an important role for the interaction between the zonal mean flow and orography. This point will be discussed further in section 6.

4. The Northern Hemisphere summer subtropical circulation

a. The North American monsoon and the Northern Hemisphere summer anticyclones

The onset of the North American monsoon is characterized by the northward extension of heavy precipitation from southern Mexico in early June to the southwestern United States in early July. In this investigation, which is interested in the gross features of the subtropical circulation, we consider the June–August season as a whole but our results will have implications for the onset and decay of monsoons. Stensrud et al. (1995) suggest that 60%–80% of the annual rainfall over northwestern Mexico occurs during the North American monsoon, with rainfall over the ''Great Plains'' tending to be out of phase with this monsoon precipitation. An interesting hypothesis is that, provided a monsoon region represents a local maximum in temperature, then isentropic downgliding and diabatic enhancement of the flow into the monsoon could imply an inhibition of rainfall over the Great Plains region. This could be an explanation for the negative correlations between North American monsoon and Texas rainfall found by Barlow et al. (1998). Rainfall farther east over the United States tends to be in phase with the monsoon (Higgins et al. 1997). Here, our heating NAm includes the effects of this eastern precipitation.

As indicated by our ''canonical'' monsoon of section 3, the large-scale low-level flow over the region is strongly related to the Pacific and Atlantic subtropical highs, with the low-level southerly jet over the Great Plains associated to a large extent with the North Atlantic subtropical anticyclone and the northwesterlies west of Baja California associated with the North Pacific subtropical anticyclone (Fig. 1a). There has been controversy over the relative importance of various moisture sources for the North American monsoon and also the relative importance of mean flow and synoptic transients for the transport of this moisture. This debate has been summarized by Adams and Comrie (1997). The debate is still not completely resolved, owing in part to the poor definition of the Gulf of California at current data product resolutions and to discrepancies between National Centers for Environmental Prediction (Kalnay et al. 1996), and ECMWF reanalyses (Schmitz and Mullen 1996; Barlow et al. 1998). However, Schmitz and Mullen (1996) suggest that, at the scales of interest here, it is moisture transport by the mean flow that dominates. Using ECMWF analyses, they calculated that about 80% of the moisture converging into the region 18°–40°N and 115°–97°W, which encompasses much of the subtropical North American monsoon rains (Fig. 2a), originates over the Gulf of Mexico. Variability of the Great Plains LLJ that flows off the Gulf of Mexico has been linked to summertime precipitation anomalies that have occurred over large parts of the United States and even Canada (Min and Schubert 1997). Schmitz and Mullen (1996) also suggest, however, that the Pacific is not insignificant as a source of moisture for the southwestern U.S. monsoon rains. If rapid monsoon onset suggests positive feedbacks between monsoon rainfall and the large-scale circulation, then our results will tend to support both the dominance of the Gulf of Mexico source and the secondary role of a Pacific source.

1) 1990–94 DATA

The impact of North American monsoon heating and heating over the North Pacific for June–August is now investigated with a series of experiments. First the mountains only are used and then the heating regions NAm, NPac, and the Hadley Cell (HC), highlighted in Fig. 2, are successively included. This division of heating regions was guided by the analysis of the thermodynamic balance in section 3. Box NAm encompasses the monsoon heating. The monsoon is considered here to be triggered by land–sea sensible heating contrasts and is taken as a given. This heating is deep convective in the Tropics, maximizing at 4 K day^{-1} at 400 hPa, but becomes shallower in the extratropics. NPac includes the local cooling in the region of subtropical descent. This is thought to be at least partly due to diabatic enhancement. The cooling is greater than 1 K day^{-1} between about 250 and 900 hPa, maximizing at -3 K day^{-1} at about 700 hPa. Here HC encloses the forcing in the ''local Hadley circulation'' over the ocean. This summer Hadley circulation could be influenced by the strong meridional sea surface temperature gradients that result from Ekman pumping in the subtropics. Elsewhere in each experiment, zonal-mean heating is applied.

Figure 6a shows the 674-hPa ω field at day 16 for the integration with orography only. Around 20% of the observed descent (Fig. 3a) is simulated off the west coast of North America in response to mountains only (note that the contour interval in Fig. 6a is one-half that in Fig. 3a).

Figure 6c shows the result for an integration with mountains and North American monsoon, NAm, heating applied. The descent over the eastern subtropical ocean is increased and represents about 43% of the observed descent (Fig. 3a) and about 37% of the descent seen in the full simulation (not shown). These figures are in good agreement with the analysis of the thermodynamic energy equation that suggested that about 40% of the descent in this region should be adiabatic. In particular, it suggests that *all* of the adiabatic descent can be accounted for by North American monsoon heating and orographic forcing.

When the local cooling, NPac, is included, the descent at 674 hPa doubles (Fig. 6e). The horizontal position and vertical structure of the descent are little changed from the previous simulation, and this is further evidence for concluding that the NPac local cooling is at least partly a response to the remotely forced adiabatic

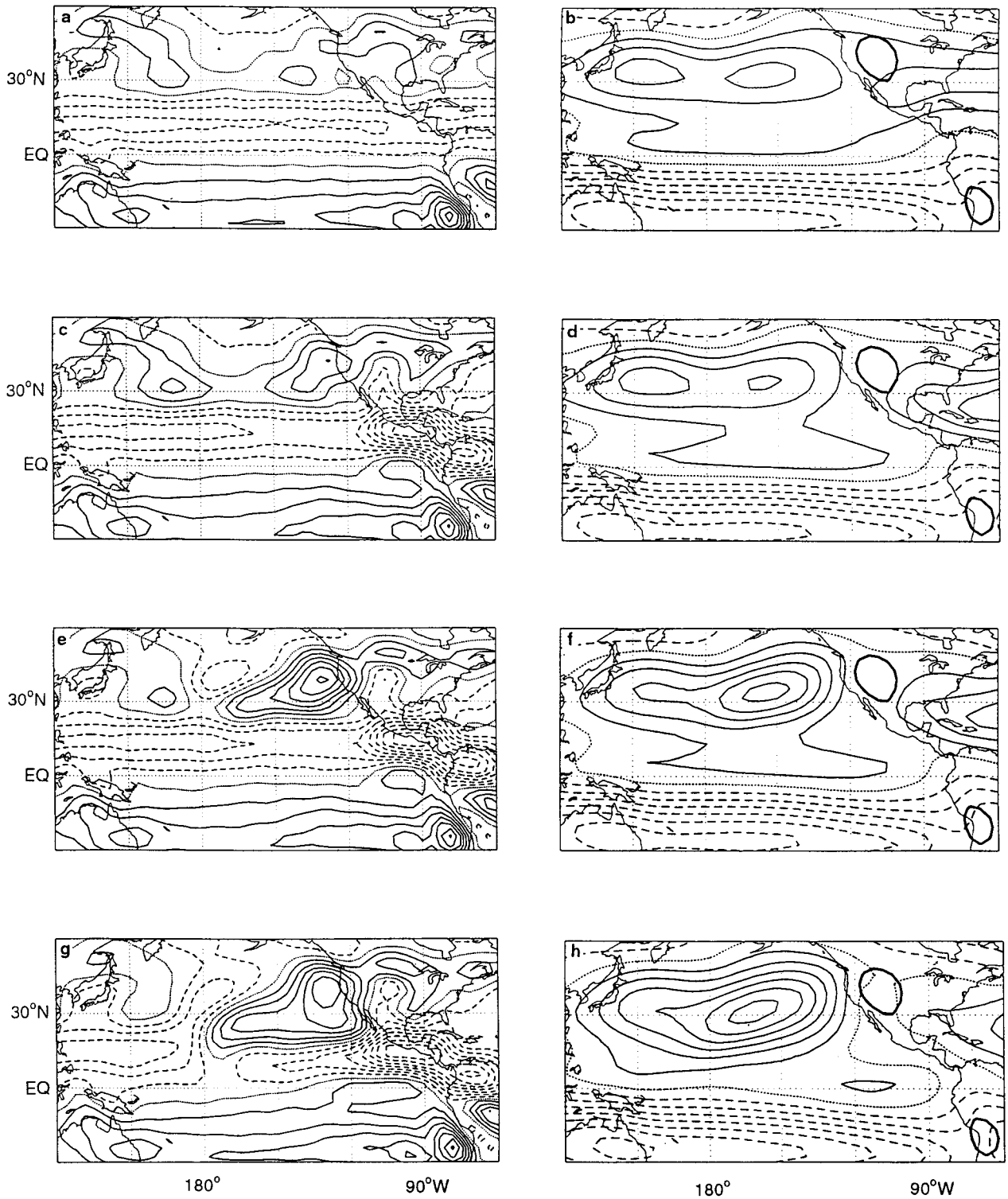

FIG. 6. (a),(c),(e),(g) Vertical velocity ω at 674 hPa and (b),(d),(f),(h) horizontal streamfunction at 887 hPa for Jun–Aug based on the 1990–94 climatology. (a),(b) A model simulation with mountains only. (c),(d) A simulation with mountains + NAm heating. (e),(f) A simulation with mountains + NAm + NPac heating. (g),(h) A simulation with mountains + NAm + NPac + HC heating. Day 16 is shown. The contour interval for ω is 0.25 hPa h^{-1} and for the streamfunction is 2×10^6 m^2 s^{-1}. Positive contours are solid, the zero contour is dotted, and negative contours are dashed. The intersection between the orography and the 887-hPa surface is shown with thick contours.

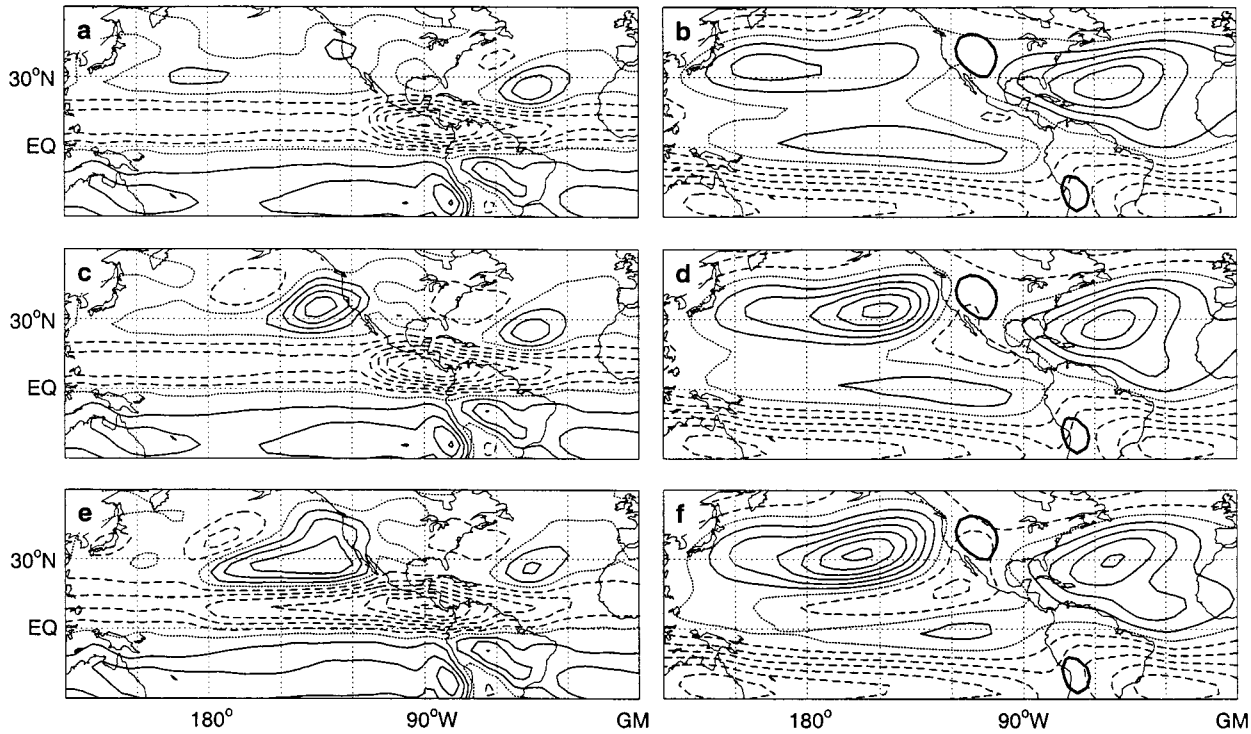

FIG. 7. (a),(c),(e) Vertical velocity ω at 674 hPa and (b),(d),(f) horizontal streamfunction at 887 hPa for Jun–Aug based on the ERA climatology. (a),(b) A simulation with mountains + NAm heating. (c),(d) A simulation with mountains + NAm + NPac heating. (e),(f) A simulation with mountains + NAm + NPac + HC heating. Day 16 is shown. The contour interval for ω is 0.5 hPa h^{-1} and for the streamfunction is 2×10^6 m^2 s^{-1}. Positive contours are solid, the zero contour is dotted, and negative contours are dashed. The intersection between the orography and the 887-hPa surface is shown with thick contours.

descent. The overall magnitude of the subtropical descent (Fig. 6e) is comparable to the observed descent (Fig. 3a). The cooling does lead to a lowering of the level of maximum descent from about 400 hPa in the NAm simulation to about 500 hPa in the NAm + NPac simulation. Assuming that the vertical profile of our cooling is reasonable, this implies that a better representation of orography may be required to attain the observed maximum descent level of around 700 hPa.

Next, the ''local Hadley cell'' forcing, HC, is applied. The analysis of the observed thermodynamic balance suggested that this forcing would result in a southward extension of the descent region, and this is precisely what happens (Fig. 6g). This forcing has almost no impact farther north.

Last, the diabatic forcing over the west Pacific (0°–60°N, 120°–180°W; not shown) is found to have a strong local effect, increasing the ascent there, but has little impact on the descent over the eastern subtropical North Pacific.

At 35° latitude, and assuming $\omega = 0$ at the surface, Sverdrup balance would imply that 0.25 hPa h^{-1} descent at 674 hPa would be accompanied by about 1 m s^{-1} equatorward flow at 887 hPa. This is indeed the case for all the experiments in the series and emphasizes that Sverdrup balance is operating. Hence the reader can readily determine the meridional motion from the ω results given.

Mountains alone do lead to some closing off of the North Pacific subtropical anticyclone (Fig. 6b). The eastern flank of the anticyclone is significantly enhanced by the inclusion of the North American monsoon (Fig. 6d). The North Pacific cooling (thought to be the diabatic enhancement) tends to strengthen the anticyclone over the eastern Pacific (Fig. 6f). The ''Hadley cell'' forcing (Fig. 6h) leads to further improvements in the simulation of the equatorward flank of the North Pacific subtropical anticyclone (cf. Fig. 1a). The west Pacific forcing leads to improvements over the west Pacific (not shown, but as in Fig. 4b).

The North American monsoon has a strong impact on the western side of the North *Atlantic* subtropical anticyclone (Fig. 6d) giving southerly flow from the Gulf of Mexico into North America. However, this is not as strong as seen in the observations (Fig. 1a) and may imply that this monsoon cannot induce sufficient moisture inflow to be consistent with its heating. Later it will be demonstrated that the Asian monsoon acts to augment the lower-tropospheric flow from the subtropical North Atlantic into Central and North America, perhaps influencing the moisture supply to the North American monsoon.

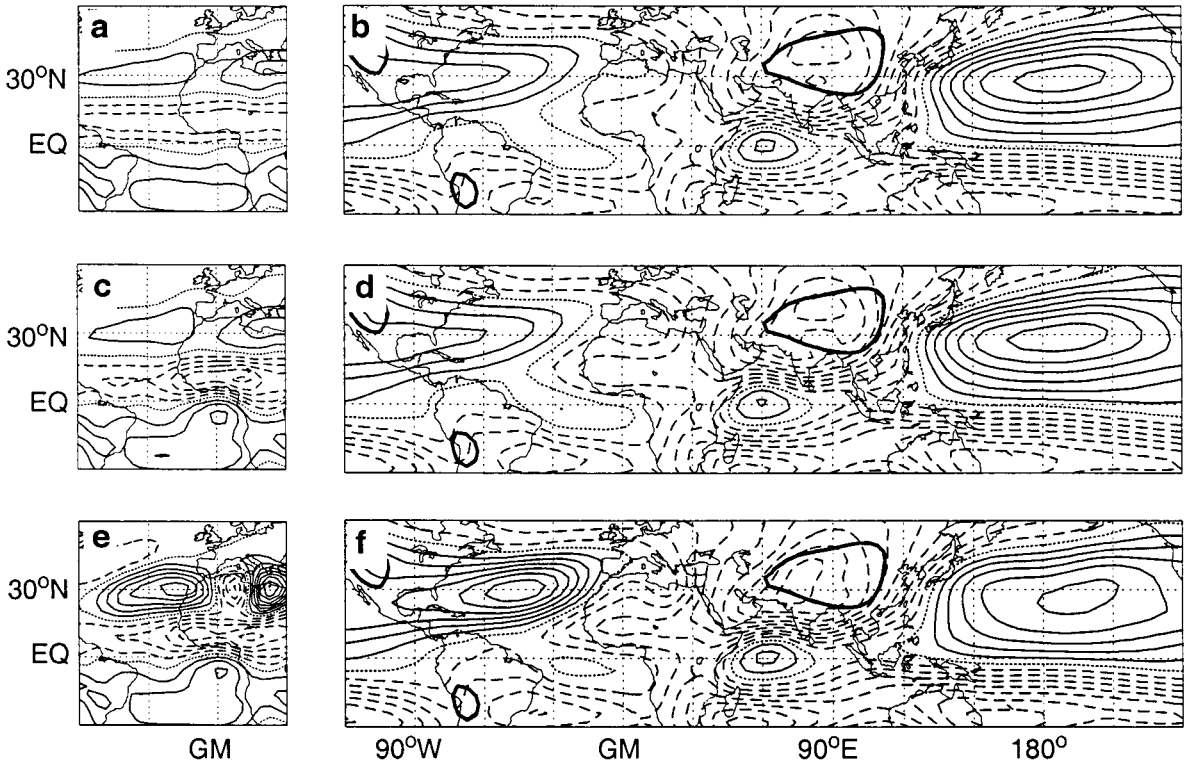

FIG. 8. (a),(c),(e) Vertical velocity ω at 674 hPa and (b),(d),(f) horizontal streamfunction at 887 hPa for Jun–Aug based on the ERA climatology. (a),(b) A simulation with mountains + A heating. (c),(d) A simulation with mountains + A + NAf heating. (e),(f) A simulation with mountains + A + NAf + NAtl heating. Day 16 is shown. The contour interval for ω is 0.5 hPa h^{-1} and for the streamfunction is 2 $\times 10^6$ m^2 s^{-1}. Positive contours are solid, the zero contour is dotted, and negative contours are dashed. The intersection between the orography and the 887-hPa surface is shown with thick contours.

Although the combined effect of North American monsoon heating, local subtropical cooling, and Hadley forcing is a strengthening of the subtropical anticyclone over the eastern North Pacific, they have little effect over the western North Pacific (Figs. 6d,f,h). Hence, these features are not expected to influence the low-level flow into the Asian summer monsoon.

2) ERA 1979–93 DATA

The ERA data have been used to investigate the sensitivity of our results to the precise form of the diabatic forcing (and basic state) and to extend the analysis to other ocean basins.

The ERA results for mountains + NAm, mountains + NAm + NPac, and mountains + NAm + NPac + HC are given in Fig. 7. It is found that differences between the 1990–94 and ERA climatologies are not important for the final comparison between the model results and the observations. In addition, the change in zonal mean basic state has almost no effect on the integrations. There does, however, appear to be some sensitivity to the diabatic forcing changes that may have many implications such as for the simulation of marine cloud in GCMs. The mountains + ERA NAm heating induce around 28% of the descent seen in the full simulation (cf. Figs. 7a and 4a) as compared with the 37% figure for the 1990–94 heating. The ERA North Pacific cooling increases the magnitude of the descent by a factor of 3.5 (cf. Figs. 7a,c), which is larger than the doubling found in the 1990–94 results. ERA HC forcing tends to offset the increased intensification somewhat (cf. Figs. 7c,e).

The low-level flow over the North Atlantic and into North America is still only about 70% of that in the full simulation (Fig. 4b). Although it is more comparable to the observations (Fig. 1a), it could be argued that the better comparison is with the control simulation. This again suggests that not all the flow of moist air into the North American monsoon is directly forced by it.

b. The Asian and North African monsoons and the Northern Hemisphere summer anticyclones

Here, we look at the impact of the Asian and North African monsoons on the Northern Hemisphere subtropical circulation. First we apply the Asian monsoon heating, A, (Fig. 2a). Note that the 150 W m^{-2} contour in A delimits well the ''Southeast Asian monsoon'' and ''Western North Pacific monsoon'' regions identified through winter-to-summer changes in outgoing longwave radiation (Murakami et al. 1999).

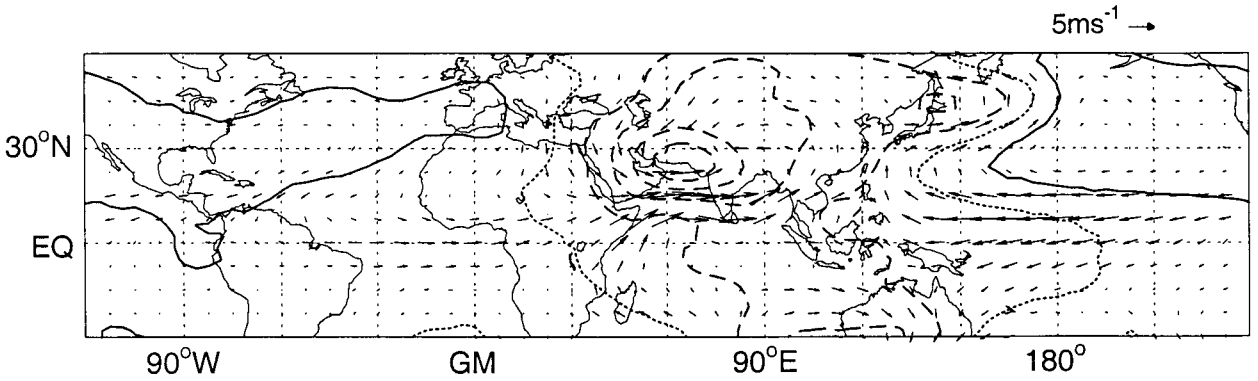

FIG. 9. Surface pressure and 887-hPa horizontal wind anomalies calculated as the difference between the mountain + ERA A simulation and the mountain-only simulation at day 16. The contour interval is 2 hPa. Positive contours are solid, the zero contour is dotted, and negative contours are dashed.

The Asian monsoon forcing alone induces some very realistic low-level circulation features (Fig. 8b), including cross-equatorial flow off the east coast of Africa (91% of the full simulation) and a North Pacific subtropical anticyclone (the zonal gradient of the 887-hPa streamfunction at 30°N over east Asia is equal to that in the control simulation, Fig. 4b). The moisture fluxes associated with these circulation features have been argued as being essential for sustaining the large-scale monsoon (Saha 1970; Kishtawal et al. 1994; Murakami and Matsumoto 1994). It would appear that the Asian monsoon does induce the low-level circulation with associated moisture fluxes that are consistent with its heating.

To understand better how the Asian monsoon forces the anticyclone to its east, we show in Fig. 9 the change in the lower-tropospheric flow associated with A. The poleward anomalous flow between about 10°–40°N and 90°–150°E is associated with the Sverdrup vorticity balance, mentioned in section 3, and, over the Pacific, this forms the western flank of the North Pacific subtropical anticyclone. The strengthened easterlies in the equatorial Pacific form the southern flank of this anticyclone. These wind anomalies show close similarities to the analytical results of Gill (1980) and would appear to be identifiable with the equatorial Kelvin wave solution to Asian monsoon heating. As with a Kelvin wave, the equatorial flow induced to the east of 150°E has little meridional wind component (Fig. 9) and, in the absence of the North American monsoon, is not efficiently ''closed off'' at the American west coast. Instead, the anticyclone extends as far east as the North Atlantic region (Fig. 8b). Hence there appears to be a strong zonal wavenumber 1 response to Asian monsoon heating that may contribute to North American monsoon inflow (although the maintenance of the zonally symmetric circulation in the model may play a part in this result).

As with RH, heating A induces descent to its west (Fig. 8a shows part of the region of this effect). The locations of the descent centers agree with where the orography alone places them (Fig. 4a) but the magnitude is almost doubled from 0.45 to 0.80 hPa h^{-1}. There is also a strengthening of the equatorward flow in the same location from about 1.1 to 1.7 m s^{-1}.

When the North African monsoon heating, NAf, (Fig. 2a) is included in our simulation (Figs. 8c,d), there appears to be a local Hadley circulation induced with descent to the south of the equator. Consistent with RH, this forcing is too near the equator to have a very significant impact on the subtropical circulation in the context of the physics represented by this model. For example, there is only a 10% strengthening of the descent over the eastern subtropical North Atlantic and a similarly small enhancement of the equatorward flow there.

The local cooling, NAtl, does have a major impact and leads to a trebling of the descent (Fig. 8e) and a significantly enhanced North Atlantic subtropical anticyclone (Fig. 8f). This anticyclone, however, is not sufficiently closed off at the North American east coast—the Central and North American heating is required to do this. Nevertheless, it is clear that local cooling over the eastern subtropical North Atlantic, again viewed as partly a response to *Asian* monsoon forcing, may also be important for the low-level inflow into the North American monsoon.

5. The Southern Hemisphere summer subtropical circulation

We now turn to the Southern Hemisphere summer (December–February) to study the effect of the South American monsoon. Summertime subtropical heating over South America (Fig. 2b) is significant, with the 150 W m^{-2} contour extending well beyond 30°S. As with the other monsoons and in agreement with vorticity considerations, there is a low-level jet (Min and Schubert 1997), often known as the South American or ''Pampas'' LLJ (Paegle 1984), which would appear to be associated with the South Atlantic subtropical anticyclone and which flows southward along the east side of the Andes. Although this jet is less well quantified

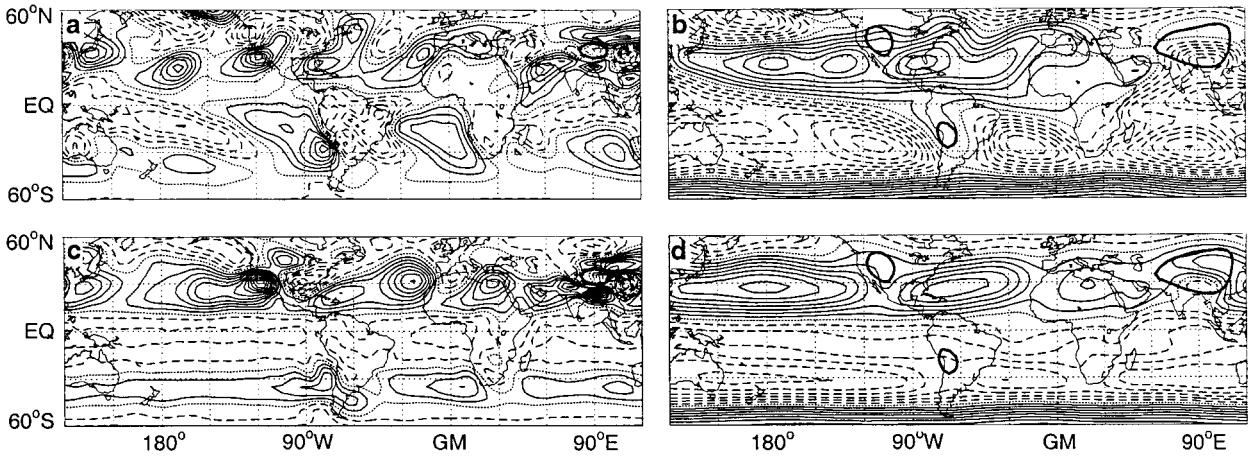

FIG. 10. As in Fig. 4 but for the Dec–Feb season. The mean of days 10–16 is shown.

or documented than its North American counterpart (Wang and Paegle 1996), it has been related to summer precipitation as far south as 35°S (Min and Schubert 1997; Nogues-Paegle and Mo 1997). Tree-ring data from northwestern Argentina suggest that the increased precipitation seen there over the last three decades is unprecedented in the last 200 yr and that this is associated with enhanced moisture transport by the Pampas LLJ (Villalba et al. 1998).

Despite the strong Northern Hemisphere winter westerlies interacting with the topography, our time integration technique does yield a reasonable solution to global orography and December–February heating, though it is a little noisy in the Northern Hemisphere. For displaying the control simulation, we take an average of days 10–16 to smooth over some of the synoptic variability. Without realistic transient fluxes of heat and vorticity, the Northern Hemisphere circulation is not as well simulated as it was in the summer. However, aspects of the flow over the two ocean basins are captured. The circulation in the Southern Hemisphere (Fig. 10b) is much more stable and compares well with the observations (Fig. 1b).

Figures 10c,d show the response to only orographic forcing using the December–February zonal-mean basic state. Again, this is displayed as an average of days 10–16. In the Southern Hemisphere, the locations of the subtropical descent, to the west of each continent, agree very well with those of the control simulation (Fig. 10a) although the magnitudes are reduced by a factor of 3 or 4 (note that the contour interval in Fig. 10c is one-half that in Fig. 10a). The subtropical anticyclones in the Southern Hemisphere (Fig. 10d) show signs of localization over the oceans but not nearly to the extent that they do in the control integration (Fig. 10b). Again, it would appear that monsoon forcing is required.

Over each of the southern continents December–February heating extends poleward to 30°S or farther and there is cooling off the western coasts (Fig. 2b). In particular these regions are isolated for South America by the boxes shown. Although the Andes alone have a significant impact on the adiabatic descent over the eastern subtropical South Pacific even in summer (Fig. 10c), the addition of SAm (Fig. 11a) strengthens this descent by around 70% (note the change in contour interval). This adiabatic descent accounts for about 42% of the total descent seen in the control simulation (Fig. 10a). Consistent with Sverdrup balance of a steady flow, equatorward flow is also strongly increased from 2 m s^{-1} in the mountain only case to 4 m s^{-1} when forced with the South American monsoon.

There is near-perfect alignment at 28°S, 79°W of the centers of strong adiabatic descent (Fig. 11a), equatorward flow (not shown), and cooling (Fig. 2b). Since the model with SAm heating alone has no information about the cooling, this agreement again adds weight to our hypothesis that the monsoon and mountains together are not only responsible for the adiabatic descent, but also lead to some diabatic descent through the diabatic enhancement mechanism.

The South Atlantic subtropical anticyclone is as strong with SAm forcing (Fig. 11b) as it is in the control simulation (Fig. 10b) and in the observations (Fig. 1b). This suggests that the monsoon-forced Kelvin wave response is of primary importance for the summertime existence of the South Atlantic subtropical anticyclone. The observed LLJ that transports moisture from the equatorial Atlantic into South America and then southward along the eastern flanks of the Andes is well simulated—implying that this monsoon induces sufficient moisture inflow to be consistent with its latent heating. Note that the South Atlantic subtropical anticyclone is not well closed off at the west coast of southern Africa. Southern African monsoon heating (Fig. 2b) would be required to achieve this. With SAm heating, the South Pacific subtropical anticyclone is also intensified (cf. Figs. 11b with 10d) and the wind stress curl over the South Pacific is strengthened.

When the diabatic cooling, SPac, is applied, descent over the eastern subtropical South Pacific increases from

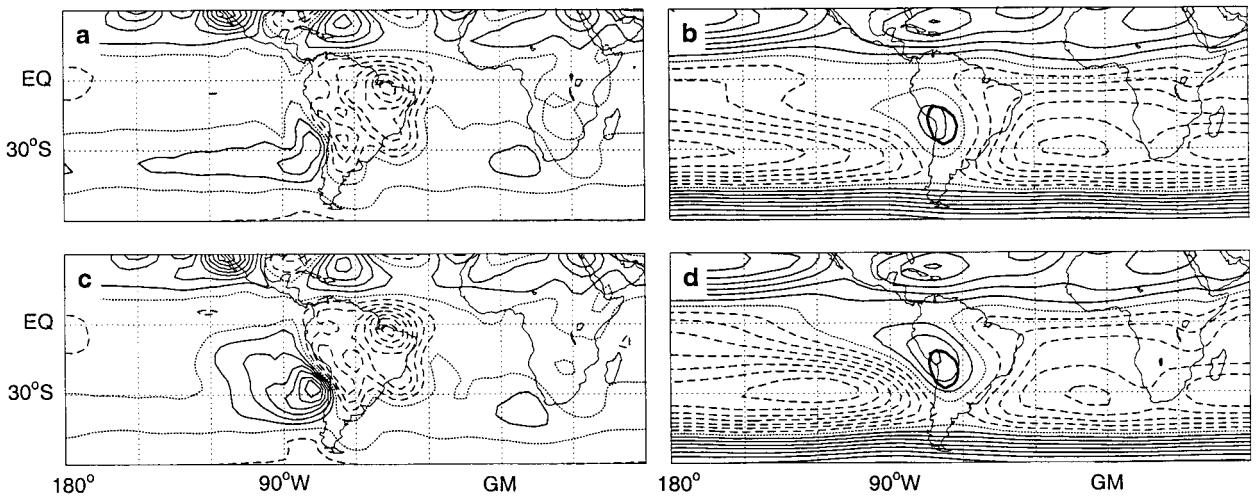

FIG. 11. (a),(c) Vertical velocity ω at 674 hPa and (b),(d) horizontal streamfunction at 887 hPa for Jun–Aug based on the ERA climatology. (a),(b) A simulation with mountains + SAm heating. (c),(d) A simulation with mountains + SAm + SPac heating. Day 16 is shown. The contour interval for ω is 0.5 hPa h^{-1} and for the streamfunction is 2×10^6 m^2 s^{-1}. Positive contours are solid, the zero contour is dotted, and negative contours are dashed. The intersection between the orography and the 887-hPa surface is shown with thick contours.

1.25 to 3.25 hPa h^{-1} (cf. Figs. 11a,c), the latter being the same as in the control integration. Associated with this in the lower troposphere, the meridional wind increases from 4 to 7 m s^{-1}. A local minimum in the streamfunction is found at around 30°S, 120°W, just as in the control integration (Fig. 10b) and in the observations (Fig. 1b), and the wind stress curl over the South Pacific is further strengthened.

6. The effect of orography

The previous sections have shown that mountains do have an impact on the subtropical circulation in summer. In particular, they appear to play a major role in the localization of the descent. In the Southern Hemisphere summer, between one-quarter and one-third of the full descent over the eastern subtropical oceans is accounted for by the mountains alone (cf. Figs. 10a,c, noting the different contour interval). In winter, the mean westerly flow strengthens and shifts equatorward. This leads to stronger subtropical interactions between the zonal-mean flow and the mountains in winter than summer. Since, in addition, the summer situation is more likely to be complicated by the effects of the diabatic forcing, the emphasis in this section is on the winter case. However, we stress that the mechanisms outlined are thought to be applicable, but less dominant, in the summertime.

The winter streamfunction response to mountains alone is given in Fig. 4d (Southern Hemisphere) and Fig. 10d (Northern Hemisphere). It is clear that the mountains are able to divide the winter subtropical anticyclonic belt into distinct anticyclones centered over the ocean basins. There is good similarity with the response seen in the full simulations (Figs. 4b and Fig. 10b) and in the observations (Figs. 1a,b) although baroclinic instability tends to affect the winter circulation in Fig. 10b. It may be possible, therefore, to obtain a basic understanding of the large-scale winter subtropical circulation from studying adiabatic mountain–zonal-mean flow interactions.

The mountain-only vertical motion response around the Rockies in winter (Fig. 10c) forms a ''5-pole pattern.'' To the west of the Rockies there is the subtropical center of descent and an extratropical center of ascent. To the east of the mountain range, there is an ascent region sandwiched meridionally between two descent regions. A very similar 5-pole vertical motion pattern is seen about the Andes in winter (Fig. 4c) and would suggest that this response is not too dependent on the exact configuration of the ambient winds and the mountains. The investigation below attempts to understand how orography can lead to these vertical motion and streamfunction responses.

Figure 12a represents schematically for the Northern Hemisphere what linear theory would predict for the response to a mountain. One would expect to see ascent on the ''upslopes'' (''+'' in Fig. 12a) an anticyclone over the mountain, and descent on the ''downslopes'' (''−'' in Fig. 12a). Linear simulations using the present model with mountains only do indeed produce these features. The method of linearization involves reducing the heating and orography by a factor of 10^6 so that quadratic terms within the model are reduced by a factor of 10^{12}. Output anomalies are then rescaled by a factor of 10^6. Further details are given in Hoskins and Rodwell (1995). Clearly the linear response is far from the real (nonlinear) response. In particular, the anticyclone is centered above the mountain rather than over the ocean basins.

To understand better the limitation of the linear theory, we show in Fig. 13a the observed June–August geopotential heights of isentropes at 24°S. The down-

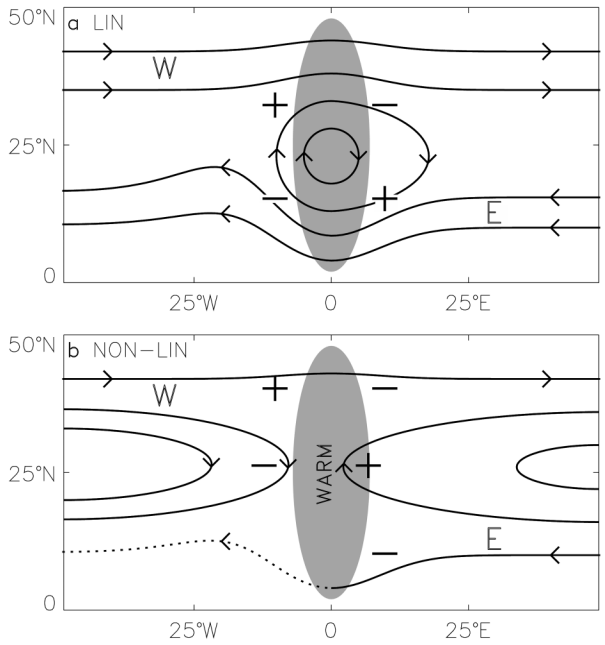

FIG. 12. Schematic diagrams depicting the adiabatic interaction between the zonally averaged flow and an idealized mountain (shaded) based on (a) linear theory in which isentropes do not intersect the mountain in the zonal plane, (b) nonlinear theory in which isentropes can intersect the mountain in the zonal plane. Contours depict low-level streamfunction. Here ''+'' indicates ascent and ''−'' indicates descent.

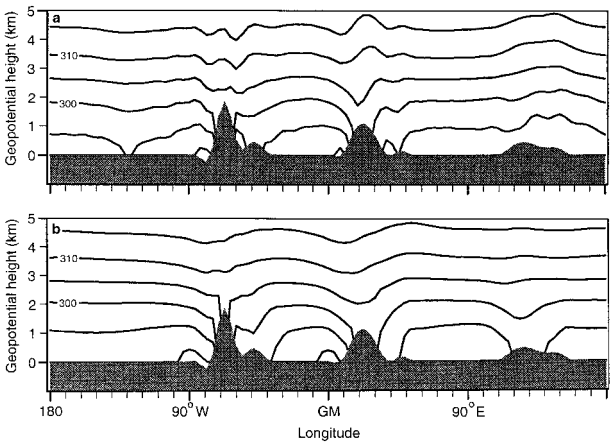

FIG. 13. Longitude–height plots at 24°S showing isentropes in winter (Jun–Aug): (a) from ECMWF analyses for 1983–88 and (b) from day 15 of a model simulation with a Jun–Aug initial state from the same analyses and forced with mountains only. The terrain profile at 24°S is also shown. The contour interval is 5 K.

ward displacement of isentropes over the mountains implies anomalously warm temperatures in these regions. Notice in particular that some isentropes intersect the mountain sides. These intersections are similar in the nonlinear model simulation with mountains only (Fig. 13b). In our linear model simulation, no such intersection can occur since the model ''sees'' a mountain one-millionth its true height.

Therefore, instead of starting from our linear situation, it is instructive to start from a situation in which the isentrope heights are constant with longitude. In this situation, isentropes will intersect the surface in the zonal, as well as the meridional, plane. Figure 12b represents schematically the response one may expect. As the low-level wintertime *easterly* trade winds (''E'' in Fig. 12b) approach the eastern slopes of the orography, they must be deflected equatorward and/or poleward since the isentrope intersects the mountain. The equatorward-deflected flow will descend on the (meridionally sloping) isentropes and be effectively blocked by the mountain. The poleward-deflected flow will rise on the isentropes and attain anticyclonic relative vorticity, implying further poleward turning. Hence, it is clear that a large proportion of the easterly flow must actually turn poleward. This is what appears to happen in reality for the case of South America (Fig. 1a). Much of the easterlies approaching southern Africa (Fig. 1a) still turn equatorward because of the effect of the Asian monsoon, but, nevertheless, there is still a clear blocking of the flow into equatorial Africa. Our model results suggest that the magnitude of the poleward flow may be somewhat sensitive to the orography used since it is simulated too strongly over southern Africa and too weakly over South America.

The poleward flow along the mountain ridge is consistent with the warm anomalies seen over the mountains in Fig. 13. Indeed, from Fig. 3, it is clear that the horizontal advection term (Fig. 3d) is the dominant term in the thermodynamic energy balance at 674 hPa over subtropical South America and is also clearly important over southern Africa. We would suggest, therefore, that horizontal advection is a major reason for the anomalous warmth (i.e., warmer than the zonal mean) of these regions in winter. To further demonstrate this effect, we have looked at our June–August mountain-only nonlinear simulation, and, indeed, anomalous lower-tropospheric temperatures in the southern subtropics match very closely the pattern of meridional motion. These results help explain why in winter Asuncion, Paraguay, is on average 4°C warmer than Antofagasta, Chile, and why Francistown, Botswana, is slightly warmer than Walvis Bay, Namibia, despite being 1 km higher in altitude. Note that Ringler and Cook (1999) applied diabatic cooling over the wintertime mountain but if this were the true driving force for the circulation, then one might expect to see these regions being anomalously *cold* in winter. However, until heating estimates from different analysis products agree better, there is room for debate about these conclusions.

The low-level flow impinging on the mountain from the west (''W'' in Fig. 12b) must also be deflected equatorward or poleward. The flow that is deflected poleward as it approaches the mountain in the extratropics rises up the sloping isentropes, it is not so effectively blocked by the mountain, and subsequently descends down the

eastern slopes. This extratropical flow is much more as suggested by linear theory and agrees better with the results of Ringler and Cook (1999). Such an extratropical flow can be seen over the Rockies (Fig. 10d) and to a lesser extent over the Andes (Fig. 4d). On the other hand, the westerly flow that turns equatorward descends on the isentropes. Below this descent, Sverdrup balance implies further equatorward flow. The full equatorward flow would appear to be essential for mass continuity if the easterly trades (E in Fig. 12b) have been effectively inhibited from crossing the mountain. The downward deflection of the isentropes toward the anomalously warm mountains (Fig. 13) may imply that the westerlies can be partially ''blocked'' to an upstream height somewhat higher than the mountain itself.

The assumption of constant isentropic height in the zonal plane would therefore appear to predict both the centering of the anticyclones over the oceans and the 5-pole vertical motion pattern. Local diabatic enhancement, among other mechanisms, will be important for subsequently explaining the correct magnitudes of each large-scale circulation feature. Indeed, diabatic enhancement may be more generally applicable and lead to an enhancement of ascent as well as descent. For example, *heating* is seen to the west of the southern tip of South America in Fig. 3b in the same location that *ascent* occurs in the mountain-only integration (Fig. 10c). Note that such heating would tend to weaken the already weak poleward deflection of the flow in this region. Clearly therefore, diabatic effects may do more than simply strengthen the mountain-forced flow. The 5-pole vertical motion pattern around the Rockies in winter (Fig. 10c), for example, is still evident but less clear in the simulation with heating (Fig. 10a).

7. Discussion and conclusions

There is a clear ''duality'' between the monsoon condensational heating and the low-level subtropical circulation in the sense that either one would be very different without the other. Nevertheless, since the monsoons are essentially an amplification of summertime land–sea *sensible* heating contrasts, their heatings have been taken as given, and the investigation has focused on *how* they affect the summer subtropical circulation. Some comments have been made on whether the lower-tropospheric circulation and in particular the flux of moist air into the monsoon regions may be consistent with the latent heating imposed there. The winter situation is quite different, and we have investigated how the interaction between the zonally averaged flow and the mountains can define much of the lower-tropospheric zonally asymmetric subtropical circulation.

The conclusions for the summer situation are the following:

- Consistent with the results of Gill (1980), the summertime low-level equatorial flank of the subtropical anticyclone to the east of a monsoon may be interpreted as a Kelvin wave response to the monsoon heat source. Hence in summer, the North Pacific subtropical anticyclone easterlies are primarily a ''response'' to Asian monsoon heating and the South Atlantic subtropical anticyclone is primarily a response to South American monsoon heating.
- A poleward-flowing low-level jet (LLJ) into and beneath the monsoon is required to satisfy low-level Sverdrup vorticity balance and would appear to be important for transporting the moisture that is required by the monsoon condensational heating. Examples of such poleward jets include the Great Plains LLJ and the Pampas LLJ. These jets close off the low-level subtropical anticyclone to the east. The North American monsoon does not appear to induce a strong enough Great Plains jet to maintain consistency between condensational heating and moisture inflow. Results suggest that the hemispheric response to the massive Asian monsoon heating may be important for augmenting the moisture inflow into Central and North America.
- The Rossby wave response to the west of subtropical summer monsoon heating, interacting with the midlatitude westerlies, produces a region of *adiabatic* descent. It has been demonstrated that such subtropical descent is induced over the eastern North Pacific by the North American monsoon, over the eastern South Pacific by the South American monsoon, and over the eastern North Atlantic by the Asian monsoon. The North African monsoon is a tropical monsoon. It is associated with a local Hadley circulation having descent in the Southern Hemisphere. In terms of the physics represented in our model, it has little impact on the subtropical descent in the Azores (or Mediterranean) region.
- The adiabatically descending air in the subtropics flows equatorward down the sloping isentropes. Furthermore, the region of equatorward flow extends to the surface, thus satisfying Sverdrup vorticity balance and tending to close off the subtropical anticyclone to the west. Such equatorward flows are seen, for example, along the Californian and Chilean coasts.
- It is speculated that the adiabatic descent will inhibit local convective heating and increase longwave cooling thus leading to a local ''diabatic enhancement'' of the monsoon-forced descent and equatorward flow. There could be positive feedbacks over the eastern subtropical oceans involving, for example, cool upwelling forced by the equatorward wind stresses. Idealized results with net cooling represented by Newtonian relaxation tend to support the idea of a local diabatic enhancement to the monsoon-forced descent. The fact that the observed cooling regions agree well with the regions of adiabatic descent forced by only the monsoon and mountains is further evidence for such a diabatic enhancement.

Hence, it can be argued that the subtropical circulation in summer can be characterized as a set of weakly interacting monsoon systems, each comprising monsoon rains, the subtropical anticyclone to the east, and the descent and equatorward flow to the west.

The order in which the mountains and heating are introduced does have a slight impact on their perceived effects. For example, when heating is introduced after the mountains, the enhanced descent generally has the same localized structure as that forced by the mountains alone. Whereas, when heating is applied without mountains, Fig. 5c, the descent it induces is less localized. In addition, one has to be mindful of the assumptions made in this study when drawing conclusions. For example, Figs. 5d,f,h show that as continental drag, Newtonian cooling, and the mountain are successively added to the simulation, the poleward monsoon inflow (the LLJ) centered at about 100°E and 700 hPa actually decreases. However, it would be wrong to argue that features such as continents and mountains lead to a weakening of the monsoon circulation since, without them, the monsoon itself would be very different (or nonexistent) (Dirmeyer 1998; Hahn and Manabe 1975; Fennessy et al. 1994; Tang and Reiter 1984).

In winter, the interaction between the zonally averaged flow and the mountains gives the essence of the zonally asymmetric subtropical circulation. The fluxes of heat and momentum by transient midlatitude systems will also play a role. Linear theory cannot explain the mountain–zonal-mean flow interaction because it centers the subtropical anticyclone over the mountains rather than over the oceans and it predicts poleward rather than equatorward flow to the west of the mountain range. An assumption of adiabatic flow and horizontal isentropes in the zonal plane appears to be a better starting point because this centers the subtropical anticyclones correctly and predicts the ''5-pole'' vertical motion pattern around the mountain range. Subsequent diabatic effects, including the local diabatic enhancement of both ascent and descent, are essential for producing the correct amplitude of the winter subtropical circulation features.

Acknowledgments. We thank Andrew Heaps, Paul Valdes, Mike Blackburn, and Brett Sconcia for their valued assistance in the production of this paper. We would like to acknowledge the Met Office and the ECMWF for their support in the preparation of this manuscript. One of the authors, MJR, would like to acknowledge the many conversations had with the late M.K. Soman, to whom this paper is dedicated.

REFERENCES

Adams, D. K., and A. C. Comrie, 1997: The North American monsoon. *Bull. Amer. Meteor. Soc.,* **78,** 2197–2213.

Anderson, D. L. T., and A. E. Gill, 1975: Spin-up of a stratified ocean, with applications to upwelling. *Deep-Sea Res.,* **22,** 583–596.

Barlow, M., S. Nigam, and E. H. Berbery, 1998: Evolution of the North American monsoon system. *J. Climate,* **11,** 2238–2257.

Dirmeyer, P. A., 1998: Land–sea geometry and its effect on monsoon circulations. *J. Geophys. Res.,* **103**, 11 555–11 572.

Fennessy, M. J., and Coauthors, 1994: The simulated Indian monsoon—A GCM sensitivity study. *J. Climate,* **7,** 33–43.

Gill, A. E., 1980: Some simple solutions for heat-induced tropical circulation. *Quart. J. Roy. Meteor. Soc.,* **106,** 447–462.

Hahn, D. G., and S. Manabe, 1975: The role of mountains in the south Asian monsoon circulation. *J. Atmos. Sci.,* **32,** 1515–1541.

Heckley, W. A., and A. E. Gill, 1984: Some simple solutions to the problem of forced equatorial long waves. *Quart. J. Roy. Meteor. Soc.,* **110,** 203–217.

Held, I. M., 1983: Stationary and quasi-stationary eddies in the extratropical troposphere. Theory, *Large-Scale Dynamical Processes in the Atmosphere,* B. J. Hoskins and R. P. Pearce, Eds., Academic Press, 127–168.

——, and A. Y. Hou, 1980: Nonlinear axially symmetric circulations in a nearly inviscid atmosphere. *J. Atmos. Sci.,* **37,** 515–533.

Higgins, R. W., Y. Yao, and X. L. Wang, 1997: Influence of the North American monsoon system on the U.S. summer precipitation regime. *J. Climate,* **10,** 2600–2622.

Hoskins, B. J., 1996: On the existence and strength of the summer subtropical anticyclones. *Bull. Amer. Meteor. Soc.,* **77,** 1287–1291.

Hoskins, B. J., and D. J. Karoly, 1981: The steady linear response of a spherical atmosphere to thermal and orographic forcing. *J. Atmos. Sci.,* **38,** 1179–1196.

——, and A. J. Simmons, 1975: A multi-layer model and the semi-implicit method. *Quart. J. Roy. Meteor. Soc.,* **101,** 637–655.

——, and M. J. Rodwell, 1995: A model of the Asian summer monsoon. Part I: The global scale. *J. Atmos. Sci.,* **52,** 1329–1340.

——, R. Neale, M. J. Rodwell, and G.-Y. Yang, 1999: Aspects of the large-scale tropical atmospheric circulation. *Tellus,* **51A-B,** 33–44.

Hourani, G. F., 1951: *Arab Seafaring in the Indian Ocean in Ancient and Earley Medieval Times.* Princeton University Press, 140 pp.

Josey, S. A., E. C. Kent, and P. K. Taylor, 1998: The Southampton Oceanography Centre (SOC) ocean–atmosphere heat, momentum and freshwater flux atlas. Southampton Oceanography Centre Rep. 6, 55 pp. [Available from Southampton Oceanography Centre, European Way, Southamton, SO14 3ZH, United Kingdom.]

Kalnay, E., and Coauthors, 1996: The NCEP/NCAR 40-Year Reanalysis Project. *Bull. Amer. Meteor. Soc.,* **77,** 437–471.

Kishtawal, C. M., N. Gautam, S. Jaggi, and P. C. Pandey, 1994: Surface-level moisture transport over the Indian Ocean during southwest monsoon months using NOAA/HIRS data. *Bound.-Layer Meteor.,* **69,** 159–171.

Klein, S. A., and D. L. Hartmann, 1993: The seasonal cycle of low stratiform clouds. *J. Climate,* **6,** 1587–1606.

——, ——, and J. R. Norris, 1995: On the relationships among low-cloud structure, sea surface temperature and atmospheric circulation in the summertime northeast Pacific. *J. Climate,* **8,** 1140–1155.

Lézine, A. M., and J. Casanova, 1991: Correlated oceanic and continental records demonstrate past climate and hydrology of North Africa (0–140 ka). *Geology,* **19,** 307–310.

Lindzen, R. S., and A. Y. Hou, 1988: Hadley circulations for zonally averaged heating centered off the equator. *J. Atmos. Sci.,* **45,** 2416–2427.

Ma, C. C., C. R. Mechoso, A. W. Robertson, and A. Arakawa, 1996: Peruvian stratus clouds and the tropical Pacific circulation: A coupled ocean–atmosphere GCM study. *J. Climate,* **9,** 1635–1645.

Matsuno, T., 1966: Quasi-geostrophic motions in the equatorial area. *J. Meteor. Soc. Japan,* **44,** 25–43.

Min, W., and S. Schubert, 1997: The climated signal in regional moisture fluxes: A comparison of three global data assimilation products. *J. Climate,* **10,** 2623–2642.

Murakami, T., and J. Matsumoto, 1994: Summer monsoon over the Asian continent and western North Pacific. *J. Meteor. Soc. Japan,* **72,** 719–745.

——, ——, and A. Yatagai, 1999: Similarities as well as differences between summer monsoons over southeast Asia and the western North Pacific. *J. Meteor. Soc. Japan,* **77,** 887–906.

Neelin, J. D., and I. M. Held, 1987: Modeling tropical convergence based on the moist static energy budget. *Mon. Wea. Rev.,* **115,** 3–12.

Nogues-Paegle, J., and K. C. Mo, 1997: Alternating wet and dry conditions over South America during summer. *Mon. Wea. Rev.,* **125,** 279–291.

Paegle, J. N., 1984: First international conference on Southern Hemisphere meteorology 31 July–6 August 1983, Sao Jose Dos Campos, Brazil. *Bull. Amer. Meteor. Soc.,* **65,** 48–54.

Ringler, T. D., and K. H. Cook, 1999: Understanding the seasonality of orographically forced stationary waves: Interaction between mechanical and thermal forcing. *J. Atmos. Sci.,* **56,** 1154–1174.

Rodwell, M. J., 1997: Breaks in the Asian monsoon: The influence of Southern Hemisphere weather systems. *J. Atmos. Sci.,* **54,** 2597–2611.

——, and B. J. Hoskins, 1995: A model of the Asian summer monsoon, Part II: Cross-equatorial flow and PV behavior. *J. Atmos. Sci.,* **52,** 1341–1356.

——, and ——, 1996: Monsoons and the dynamics of deserts. *Quart. J. Roy. Meteor. Soc.,* **122,** 1385–1404.

Saha, K. R., 1970: Air and water vapour transport across the equator in western Indian Ocean. *Tellus,* **22,** 681–687.

Sardeshmukh, P. D., and B. J. Hoskins, 1988: The generation of global rotational flow by steady idealized tropical divergence. *J. Atmos. Sci.,* **45,** 1228–1251.

Schmitz, J. T., and S. L. Mullen, 1996: Water vapor transport associated with summertime North American monsoon as depicted by ECMWF analyses. *J. Climate,* **9,** 1621–1634.

Stensrud, D. J., R. L. Gall, S. L. Mullen, and K. W. Howard, 1995: Model climatology of the Mexican monsoon. *J. Climate,* **8,** 1775–1794.

Stommel, H. M., 1961: Thermohaline convection with two stable regimes of flow. *Tellus,* **13,** 224–230.

Tang, M. C., and E. R. Reiter, 1984: Plateau monsoons of the Northern Hemisphere—A comparison between North America and Tibet. *Mon. Wea. Rev.,* **112,** 617–637.

Tibbitts, G. R., 1971: *Arab Navigationin the Indian Ocean Before the Coming of the Portuguese.* Royal Asiatic Society of Great Britain and Ireland, 640 pp.

Villalba, R., H. R. Grau, J. A. Boninsegna, G. C. Jacoby, and A. Ripalta, 1998: Tree-ring evidence for long-term precipiation changes in subtropical South America. *Int. J. Climatol.,* **18,** 1463–1478.

Wang, M. Y., and J. Paegle, 1996: Impact of analysis uncertainty upon regional atmospheric moisture. *J. Geophys. Res.,* **101,** 7291–7303.

Webster, P. J., 1987: The elementary monsoon. *Monsoons,* J. S. Fein and P. L. Stephens, Eds., Interscience, 3–32.